ARTICLE

Low-Temperature CO Oxidation on Ni(111) and on a Au/Ni(111) Surface Alloy

Jan Knudsen,[†,⊥] Lindsay R. Merte,[†] Guowen Peng,[‡] Ronnie T. Vang,[†] Andrea Resta,[§] Erik Lægsgaard,[†] Jesper N. Andersen,[§] Manos Mavrikakis,[‡] and Flemming Besenbacher[†,*]

[†]Interdisciplinary Nanoscience Center (iNANO) and Department of Physics and Astronomy, Aarhus University, DK-8000 Aarhus C, Denmark, [‡]Department of Chemical and Biological Engineering, University of Wisconsin-Madison, Madison, Wisconsin 53706, and [§]Division of Synchrotron Radiation Research, Department of Physics, Lund University, Box 118, 221 00 Lund, Sweden. [⊥]Current address: Division of Synchrotron Radiation Research, Department of Physics, Lund University, Box 118, 221 00 Lund, Sweden.

ABSTRACT From an interplay between scanning tunneling microscopy, temperature programmed desorption, X-ray photoelectron spectroscopy, and density functional theory calculations we have studied low-temperature CO oxidation on Au/Ni(111) surface alloys and on Ni(111). We show that an oxide is formed on both the Ni(111) and the Au/Ni(111) surfaces when oxygen is dosed at 100 K, and that CO can be oxidized at 100 K on both of these surfaces in the presence of weakly bound oxygen. We suggest that low-temperature CO oxidation can be rationalized by CO oxidation on O_2-saturated NiO(111) surfaces, and show that the main effect of Au in the Au/Ni(111) surface alloy is to block the formation of carbonate and thereby increase the low-temperature CO_2 production.

KEYWORDS: low-temperature CO oxidation · nickel oxide · AuNi surface alloy · low-temperature oxidation · scanning tunneling microscopy · X-ray photoelectron spectroscopy

Even though Au and Ni are bulk immiscible it has been shown that it is possible to form a surface alloy with Au atoms substituted into the surface layer on any of the low-index Ni surfaces.[1,2] These AuNi surface alloys have shown interesting catalytic properties for the steam reforming reaction ($CH_4 + H_2O \rightarrow 3\,H_2 + CO$),[1,3] where Au is shown to inhibit carbon deposition and subsequent coke formation.[1] Au/Ni has also been reported by Lahr and Ceyer[4] to catalyze low-temperature (100 K) CO oxidation. Interestingly, through a combination of high-resolution electron energy loss spectroscopy (HREELS) and mass spectroscopy these authors showed that molecularly adsorbed oxygen is stabilized on the Au/Ni(111) surface alloy at 77 K, and that this molecular oxygen is very reactive for the CO oxidation reaction at low temperature. At higher temperature (105−125 K), Lahr and Ceyer showed furthermore that the CO_2 production rate coincides with the O_2 dissociation, whereas above 125 K CO and O bound to Au react directly, resulting in CO_2 formation. However, no further experimental studies have explored low-temperature CO oxidation on the Au/Ni(111) system.

Here we have studied low-temperature CO oxidation on Ni(111), nickel oxide and the Au/Ni(111) surface alloy using a combination of scanning tunneling microscopy (STM), X-ray photoelectron spectroscopy (XPS), temperature programmed desorption (TPD), and density functional theory (DFT) calculations. We find that the chemisorbed CO and O on Ni(111) and on Au/Ni(111) do not react to form CO_2 at temperatures between 100 K and room temperature. Very interestingly, we find that both Ni(111) and Au/Ni(111) oxidize when O_2 is adsorbed at low temperatures close to 100 K and that loosely bound oxygen on the oxidized Ni(111) and Au/Ni(111) surfaces reacts with CO leading to the formation of CO_2. Our experiments reveal that CO oxidation on the oxidized Au/Ni(111) surface is qualitatively similar to that taking place on oxidized Ni(111), the primary difference being the inhibition of carbonate formation with increasing Au concentration, thus increasing the quantity of CO_2 produced at low temperature.

RESULTS AND DISCUSSION

Oxidation of Ni(111). In Figure 1 we compare the room-temperature (RT) oxidation of Ni(111) (left column) with the oxidation at ~100 K (right column). After an exposure of 40 L of O_2 at RT, islands are observed mainly at the step edges (Figure 1B), while the rest of the surface is covered by a well-ordered p($\sqrt{3} \times \sqrt{3}$)R30°-O structure (Figure 1A). The inset in Figure 1B shows a high-

*Address correspondence to fbe@inano.au.dk.

Received for review June 2, 2010 and accepted July 8, 2010.

Published online July 19, 2010. 10.1021/nn101241c

resolution STM image of one of the small islands observed near the step edge with a superimposed grid with a lattice distance of 2.95 Å, which corresponds to that of NiO(111). Upon increased oxygen exposure both the coverage of the islands and their mean apparent height increase as revealed from Figure 1B−D.

The kinetics of the RT oxidation of Ni(111) can be described as a three-stage model as discussed in the literature.[5] At low exposures (0−10 L) a p(2 × 2) structure ($^1/_4$ ML) starts to grow followed by a p($\sqrt{3} \times \sqrt{3}$) structure ($^1/_3$ ML), both of which are ordered O atom structures. Higher exposures lead to fast nucleation of NiO islands (10−40 L) followed by a slow thickening of the oxide (>40 L). The islands observed on Figure 1B,C are assigned to NiO, and our STM results are consistent with this three-stage model. The observed growth mode of the nickel oxide at RT with preferential oxidation at the step edges is, however, slightly different from the homogeneous NiO(111) clusters Kitakatsu *et al*. observed by STM after exposure to 25 L of O_2 at 300 K.[6]

The oxide structures formed after O_2 exposure at 100 K are very similar to the structures formed after RT exposure as revealed from Figure 1E,G,H. After 10 L of oxygen exposure at 100 K we observe small domains of the p($\sqrt{3} \times \sqrt{3}$)R30° structure (Figure 1E). In the boundary regions between the small domains we observe closely spaced protrusions suggesting that the coverage of oxygen in these regions is higher than that in the perfect p($\sqrt{3} \times \sqrt{3}$)R30° structure (1/3 ML). A tentative ball model of the low temperature oxygen structure is depicted in Figure 1F.

Higher oxygen exposures at 100 K lead to the growth of islands at both the upper and lower step edges. STM images of the islands recorded after an oxygen exposure of 20 and 40 L O_2, respectively, are depicted in Figure 1G,H. The height of the islands formed at 100 K is identical to the small islands observed after 40 L of oxygen exposure at RT assigned to NiO. Furthermore, the islands observed after low-temperature oxygen exposure look very similar to the NiO islands observed after RT exposure, and we thus suggest that NiO islands are formed when the Ni(111) surface is exposed to oxygen at low temperature (100 K). Upon an increase in the oxygen exposure, the coverage of the islands increases, but as Figure 1I demonstrates their apparent height is unchanged, which suggests that the formation of thicker NiO islands is kinetically limited at 100 K.

Further evidence of the formation of an oxidized Ni(111) surface at low temperature comes from the O_2 TPD spectra depicted in Figure 2A, which were acquired after O_2 was dosed at 100 K. A low-temperature desorption peak with a TPD maximum at 120 K is observed to increase with increasing low-temperature oxygen exposure. No CO or CO_2 were observed in these TPD spectra. The O_2 desorption is only observed after extensive O_2 exposures, which agrees very well with the fact that

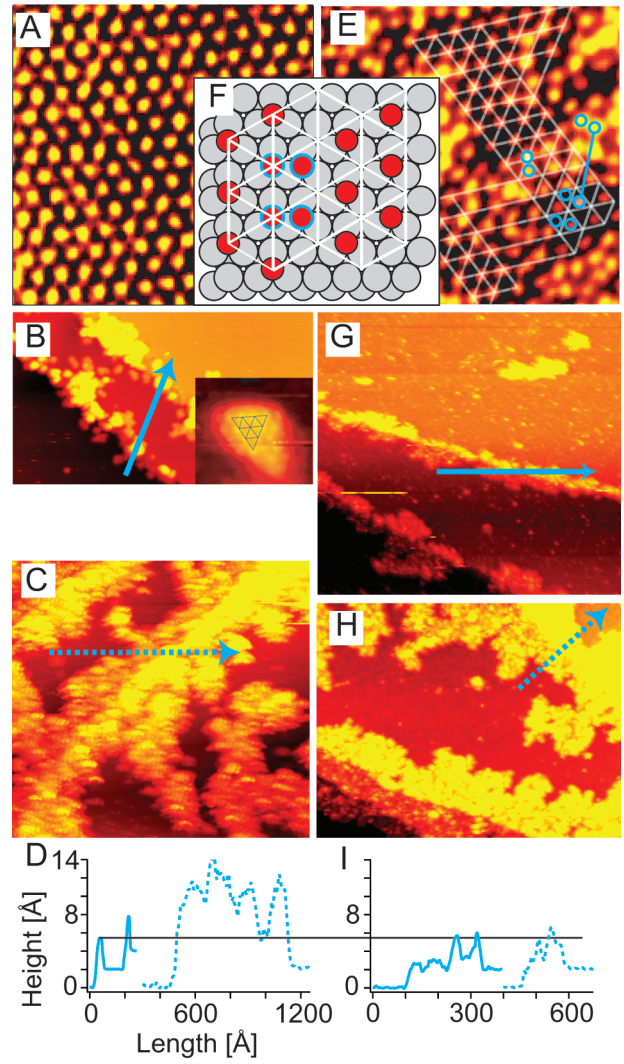

Figure 1. (A,B) STM images (70 × 70 Å^2 and 1000 × 570 Å^2) of Ni(111) exposed to 40 L of O_2 at room temperature. The small inset in panel B shows a higher resolution image of the NiO islands at the step edges. (C) STM image (1.15 nA, 743 mV, 1596 × 1486 Å^2) of Ni(111) exposed to 80 L of O_2 at room temperature. (D) Line scan along the blue arrow in panel B and the dotted line in panel C. (E) STM image (2.10 nA, 2.75 mV, 70 × 70 Å^2) of Ni(111) exposed to 10 L of O_2 at 120 K. (F) Ball model of the structure observed in panel E. The gray circles are Ni substrate atoms, and the red circles are adsorbed oxygen atoms. The blue circles correspond to the oxygen atoms marked in panel E. (G) STM image (2.2 nA, 139 mV, 800 × 740 Å^2)) of Ni(111) exposed to 20 L of O_2 at 100 K. (H) STM image (1000 × 720 Å^2) of Ni(111) exposed to 40 L of O_2 at 90 K. (I) Line scan along the blue arrow in panel G and the dotted line in panel H.

two very different structures are observed by STM depending on the oxygen exposure. From the STM and TPD results we thus suggest that the O_2 desorption peak observed after extensive oxygen exposure should be assigned to O_2 desorbing from the NiO areas. In fact, our DFT calculations indicate that the first $^1/_4$ ML of O_2 adsorbs on NiO(111) with a binding energy of −0.74 eV, whereas the differential binding energy of the second and third $^1/_4$ ML of O_2 on the same surface is −0.4 and −0.36 eV, respectively. The higher the O_2 exposures in the experiments, the more likely to probe

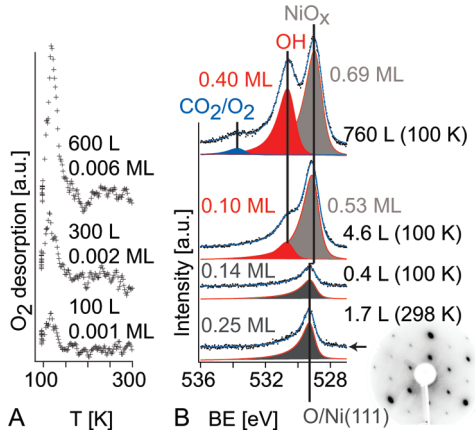

Figure 2. (A) O_2 TPD spectra of Ni(111) surfaces exposed to varying amounts of O_2 at 100 K. The heating rate was 1 K/s in all experiments. (B) O 1s spectra of Ni(111) surfaces after exposure of 0.4, 4.6, and 760 L of O_2 at 100 K. The bottom spectrum was obtained after dosing 1.7 L of oxygen onto a clean Ni(111) surface at room temperature, which leads to an almost perfect p(2 × 2) structure as evidenced by the sharp 2 × 2 low energy electron diffraction spots.

the latter two O_2 adsorbed states, leading to the low-temperature desorption peaks. A similar desorption peak with the TPD maximum at 95 K has previously been observed on Ni(100) by Kim *et al.*[7] after extensive oxygen exposure at 80 K. From an interplay of XPS, TPD, and near edge X-ray absorption fine structure (NEXAFS), these authors assigned this feature to molecular oxygen.[7] The small temperature difference of the TPD maximum reported by Kim *et al.* and the results reported in Figure 2A are most likely related to different O_2 adsorption temperatures and differences between Ni(100) and Ni(111) surfaces.

Figure 2B shows the O 1s XPS spectra for Ni(111) surfaces exposed to different amounts of oxygen at 100 K. For reference the O 1s spectrum of a p(2 × 2) structure grown at RT with an ideal coverage of 0.25 ML is shown at the bottom. We find that oxygen in the p(2 × 2) structure has a binding energy of 529.3 eV in agreement with previous studies,[8] even though higher binding energies have also been reported.[5,9] After dosing 0.4 L of oxygen at 100 K, we observe a single oxygen peak with the same binding energy as for the p(2 × 2) structure grown at RT. Consistent with our STM experiments, we thus conclude that the initial oxygen exposure at 100 K leads to a chemisorbed structure of atomic oxygen located in 3-fold hollow sites on the Ni(111) surface. After an exposure of 4.6 L of oxygen at 100 K the main oxygen peak shifts 0.14 eV toward lower binding energy, and subsequent oxygen exposure (760 L) at 100 K leads to a further downward shift of the main peak to a binding energy of 529.0 eV. The reduction of the binding energy of the main XPS peak is consistent with the formation of nickel oxide (O^{2-}).[5] In addition to the shift of the main peak a shoulder is observed at 530.7 eV at higher oxygen exposures. This shoulder, located 1.7 eV above the binding energy of nickel oxide (529.0 eV), is always observed on Ni(111) after large oxygen exposures and has previously been assigned to hydroxyl species formed from H_2 and H_2O in the residual gas.[5,8,10,11] The high binding energy peak located at 533.7 eV (4.7 eV above the peak assigned to O^{2-}) could either be assigned to molecular oxygen[7] and/or CO_2 adsorbed from the residual gas, as we observe a peak with the same binding energy after dosing CO_2 onto the Ni(111) surfaces predosed with oxygen. Given the fact that we observe O_2 desorption in the TPD experiments after extensive oxygen exposure, we assign the feature at 533.7 eV mainly to molecular oxygen.

From the known coverage (0.25 ML) of the p(2 × 2) structure it is possible to calculate the oxygen coverage corresponding to the different oxygen peaks depicted in Figure 2B. The total coverage of oxygen (NiO_x + OH) after an exposure of 760 L is 1.09 ML, which is close to the coverage of ~1.5 ML for NiO(111) and significantly higher than the coverage for chemisorbed oxygen structure.

Co-adsorption of CO and O on Ni(111). Prior to the coadsorption experiments of CO and O_2 two different reference structures of adsorbed CO on Ni(111) were characterized with XPS: A c(4 × 2)-CO structure with CO adsorbed in 3-fold hollow sites (fcc/hcp), and a ($\sqrt{7} \times \sqrt{7}$)R19°-CO structure with CO adsorbed in both on-top and bridge sites, corresponding to coverages of 0.5 and 0.57 ML, respectively. The c(4 × 2) structure was prepared by adsorption of 10 L of CO at RT, whereas the ($\sqrt{7} \times \sqrt{7}$)R19° structure was prepared by adsorption of 100 L of CO at 220 K.[9] From XPS measurements the C 1s binding energy of CO adsorbed in Ni(111) hollow (fcc/hcp), bridge, and on-top sites were determined to be 285.15, 285.25, and 285.91 eV, respectively, in excellent agreement with a previous study by Held *et al.*[9] The small chemical shift of 0.1 eV between CO adsorbed in hollow and bridge sites makes it difficult to unambiguously distinguish between these two adsorption sites, and we will therefore use the term bridge/hollow in the subsequent discussion of our XPS data.

Figure 3A shows selected C 1s spectra obtained on Ni(111) samples exposed to oxygen followed by exposure to CO. Spectrum I is recorded immediately after an initial exposure of 2 L of O_2 at ~90 K and subsequent coadsorption of 5 L of CO at ~90 K. Two peaks are observed corresponding to CO adsorbed in bridge/hollow sites and on-top sites, respectively, which is in excellent agreement with a previous XPS study of coadsorption of oxygen and CO.[9] Spectrum II in Figure 3A was recorded after flashing the CO and oxygen exposed Ni(111) sample to 273 K. A comparison of spectrum I and II clearly shows that the peak located at 285.4 eV, assigned to CO adsorbed in bridge/hollow sites, disappears after flashing.

Spectrum III in Figure 3A shows the C 1s region for a Ni(111) sample predosed with 600 L of oxygen at ~90 K and subsequently coadsorbed with 5 L of CO at

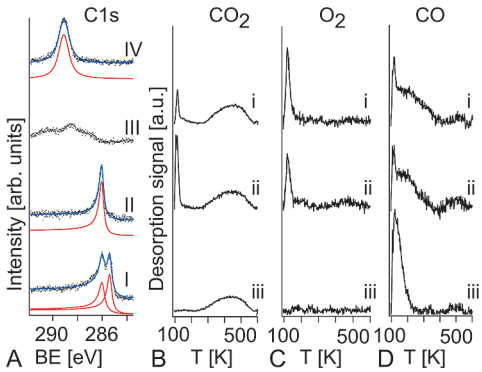

Figure 3. (A) I and III: C 1s XPS spectra obtained after 5 L of CO has been dosed onto Ni(111) predosed with with 2 L of O_2 (spectrum I) or 600 L of O_2 (spectrum III). The sample is kept at 90 K during both the gas dosing and the measurement. II and IV: C 1s spectra obtained after flashing preparation I and III, respectively, to 273 K. (B–D) CO_2, O_2, and CO TPD spectra obtained simultaneously on three different sample preparations: (i) 600 L of O_2 followed by 5 L of CO dosed at 100 K; (ii) 600 L of O_2 followed by 5 L of CO_2 dosed at 100 K; (iii) 600 L of O_2 dosed at 100 K and flashed to 150 K, followed by cooling to 100 K and subsequently dosed with 5L of CO.

~90 K. This spectrum is clearly different from the spectrum of CO adsorbed on the low-coverage O/Ni(111) surface (spectrum I), and no peaks compatible with CO molecules adsorbed in hollow, bridge, or on-top sites are observed, and neither are any sharp C 1s peaks observed. The absence of chemisorbed CO features in the XPS spectrum is unexpected on a chemisorbed oxygen structure,[9,12] and the XPS experiments thus support the formation of a nickel surface oxide at low temperature, in agreement with the low-temperature STM measurements and TPD spectra presented above. Upon flashing this sample to 273 K, a sharp peak develops with a C1s binding energy of 289.1 eV. A similar carbon peak with a C 1s binding energy of 289 eV has previously been assigned to carbonate (CO_3^{2-}) on a Ni(100) surface exposed to O_2/CO_2 mixtures.[13] The peak at 289.1 eV is, therefore, assigned to carbonate formed from the carbon species, which gives rise to the broad peaks in spectrum III. The observation of carbonate (CO_3^{2-}) on the surface after direct flashing proves that the NiO phase is able to react with adsorbed CO.

In summary, the oxygen coverage found in the XPS experiments, the different adsorption behavior of CO on O/Ni(111) with high and low coverage of oxygen, the low-temperature STM experiments, and the O_2 desorption peak observed on O/Ni(111) samples with a high oxygen coverage all suggest that NiO is formed when Ni(111) is saturated with oxygen at temperatures around ~100 K. Previous HREELS and Auger electron spectroscopy (AES) experiments have shown that electrons from 5 to 2 keV can stimulate oxidation at 120 K on Ni(111).[14] The XPS spectra described above were, however, recorded directly after one single oxygen exposure, and the photoelectrons cannot therefore increase the overall oxygen coverage.

Figure 3B–D shows the CO_2, O_2, and CO TPD desorption spectra recorded after three different sample preparations. Sample i was prepared by dosing 600 L of O_2 at 100 K followed by 5 L of CO at the same temperature. Two desorption peaks located at ~120 and ~420 K are clearly visible in the CO_2 desorption spectrum of this surface. The broad desorption peak at 420 K is assigned to the decomposition of carbonate both in agreement with the XPS result described above and TPD studies from the literature.[13,15] The low-temperature CO_2 desorption peak in spectrum i is assigned to direct desorption of CO_2. This assignment is supported by the CO_2 desorption spectrum shown in spectrum ii, which is obtained after direct CO_2 dosing at 100 K onto Ni(111) saturated with 600 L of oxygen at 100 K. A large low-temperature CO_2 desorption feature is clearly visible in this spectrum, and this feature is thus assigned to adsorbed CO_2 on the NiO surface. A comparison of the CO_2 and O_2 desorption peaks depicted in Figure 3B,C clearly demonstrates that the low-temperature CO_2 desorption peak is only observed when O_2 desorbs simultaneously. Spectrum iii is recorded on a Ni(111) sample prepared by carrying out quick flash to 150 K between the O_2 and CO dosing such that weakly bound oxygen desorbs before CO is dosed. CO_2 desorption from carbonate decomposition is again observed at 420 K in this spectrum, but no CO_2 is observed to desorb at low temperature when weakly bound oxygen is absent. Without weakly bound oxygen, adsorbed CO desorbs directly at 120 K rather than being oxidized to CO_2. This conclusion is supported by the CO desorption spectra shown in Figure 3D, which show an increased intensity of the low-temperature CO TPD peak of spectrum iii. A very similar low-temperature TPD CO peak was observed by Guo *et al.*, when CO is adsorbed on a nickel oxide grown on a Ni(111) surface, and this CO peak was therefore assigned to CO desorbing from a nickel oxide.[16]

If the order of the CO and O_2 dosing is reversed so that 5 L of CO is dosed first followed by 600 L of oxygen at 100 K, no O_2 or CO_2 desorption is observed. Only CO is observed to desorb, and the spectrum is similar to the spectrum of a CO saturated Ni(111) surface. Thus, no reactivity at all is observed on the CO covered Ni(111) surface. This conclusion is furthermore verified by XPS experiments, which show no change in the O 1s or C 1s spectra when the CO covered Ni(111) is exposed to O_2 at 90 K.

In summary, the TPD experiments show that CO molecules react with a Ni(111) surface oxidized at 100 K. If weakly bound oxygen is present on the surface, a fraction of the CO molecules are oxidized to CO_2 desorbing at ~120 K, and another fraction of CO molecules form carbonate, which leads to CO_2 desorption at ~420 K. If, on the other hand, weakly bound oxygen is absent on the surface, no low-temperature CO_2 desorption is observed, but CO_2 desorption is observed at the

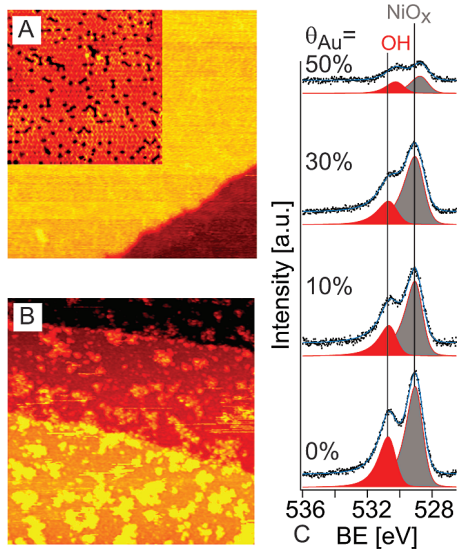

Figure 4. (A) STM image (400 × 400 Å²) of the Au/Ni(111) surface alloy with 3% Au atoms in the surface layer. The small inset (120 × 120 Å²) shows the Au atoms in the surface layer as dark depressions. (B) The Au/Ni(111) surface alloy from panel A after exposure to O_2 at 100 K for 100 s. (C) O 1s spectra taken after an exposure of 50 L of oxygen at 90 K to samples with different Au coverages. The Au coverages are given in the figure.

temperature where carbonate is known to decompose. The CO precovered Ni(111) surface is not reactive toward CO_2 formation; apparently, preadsorbed CO molecules completely block oxygen adsorption.

Oxidation of Au/Ni(111) Surface Alloy. By evaporating Au onto a Ni(111) surface, it has been previously shown that it is possible to form a Au/Ni(111) surface alloy, where the topmost surface Ni atoms are partly substituted with single Au atoms.[1,2] Here, we have studied the effect of Au concentration in the Au/Ni(111) surface alloy on the low-temperature CO oxidation.

Figure 4A shows STM images of a Au/Ni(111) surface alloy with approximately 3% of Au atoms substituted into the topmost surface layer of Ni(111). In atomically resolved images Au atoms appear as dark depressions as shown in the inset in Figure 4A, and the Au coverage in the surface layer can thus easily be determined by simply counting the Au atoms. The STM images, in general, reflect a detailed convolution of electronic and geometric structures, that is, the local density of states at the Fermi level, and that is why Au appears as depressions in the high-resolution images. Figure 4B depicts the Au/Ni(111) surface alloy in Figure 4A after exposure of 10 L of O_2 at 100 K. Small islands are observed all over the surface. These islands are similar to the NiO islands observed on the oxygen exposed Ni(111) surfaces shown in Figure 1 G,H, and we therefore conclude that NiO is also formed on the 3% Au/Ni(111) surface alloy. A comparison between Figure 1G,H and Figure 4B reveals, however, that NiO islands are formed preferentially along the step edges on the clean Ni(111) surface in contrast to the 3% Au/Ni(111) surface alloy where NiO islands form both on the terraces and along the step edges. Au atoms alloyed into the Ni(111) surface thus seem to facilitate NiO formation on the terraces at low temperature.

Figure 4C shows XPS spectra of the O 1s region for the Au/Ni(111) surface alloys with an increasing Au coverage after exposure of 50 L of oxygen at 90 K. In these experiments the surface was exposed to oxygen by means of a doser, and we estimate that the local pressure and hence the effective exposure is approximately 10 times higher than the 50 L estimated from the background pressure. Similar to the case for the oxygen exposed Ni(111) surface, we observe two XPS peaks with binding energies of 529.1 eV (NiO_x) and 530.7 eV (OH), respectively. The Au coverage does not have any detectable effect on the position of these two oxygen XPS peaks up to a Au-coverage of 0.3 ML. Both peaks shift, however, 0.3−0.4 eV toward lower binding energies for the 0.5 ML Au/Ni(111) surface alloy. The small XPS peak observed at 533.7 eV and assigned to molecular oxygen on clean Ni(111) is not detectable in the spectra from Au/Ni(111) surfaces exposed to oxygen (Figure 4C), but we cannot exclude the existence of molecular oxygen on oxidized Au/Ni(111) surfaces. In contrast to the binding energies, the oxygen coverage is clearly affected by the Au coverage as seen from Figure 4C. The saturation coverages of oxygen on the 10% and 30% Au/Ni(111) surface alloys are 0.81 and 0.76 ML, respectively. This high oxygen coverage is incompatible with a chemisorbed oxygen structure and instead suggests a structure with patches of NiO coexisting with either single Au atoms and/or small Au clusters. This conclusion agrees well with the fact that the binding energies of both O 1s peaks are identical to the energies for the oxidized Ni(111) surface.

In conclusion, the combination of STM and XPS reveals that the oxide formation on Ni(111) and Au/Ni(111) is indeed very similar, the only difference between them is that Au atoms facilitate NiO formation at the terraces and reduce the overall oxygen coverage.

Co-adsorption of CO and O on the Au/Ni(111) Surface Alloy. Figure 5A shows the CO_2 desorption spectra for the Au/Ni(111) surface alloys exposed to 300 L of O_2 followed by 5 L of CO at 100 K. The low-temperature CO_2 TPD desorption peak is clearly observed to increase with Au coverage, whereas the CO_2 desorption peak assigned to carbonate decomposition at 420 K decreases with increasing Au coverage. The effect of Au is thus to block the formation of carbonates, leading to an increased amount of CO_2 desorbing at low temperature. No CO_2 desorption is observed in the TPD spectrum when a CO saturated Au/Ni(111) surface alloy is exposed to oxygen at 100 K.

The reduced carbonate formation on the oxygen-covered Au/Ni(111) surface alloys exposed to CO is supported by the XPS spectra shown in Figure 5B. These spectra were recorded on Au/Ni(111) surface alloys ex-

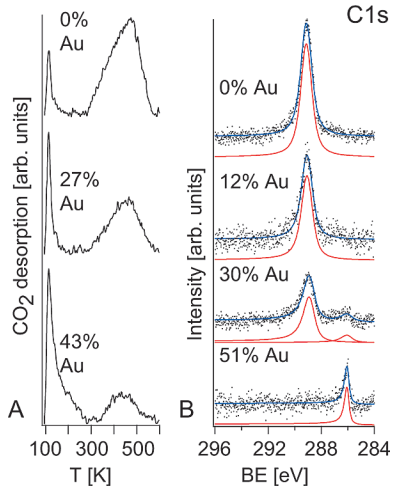

Figure 5. (A) CO_2 desorption spectra of Au/Ni(111) surface alloys exposed to 300 L of O_2 followed by 5 L of CO at 100 K for different Au coverages (given in the figure). (B) C 1s XPS spectra of Au/Ni(111) surface alloys exposed to 600 L of O_2 followed by 5 L of CO at 90 K and subsequently flashed to 273 K.

posed to 600 L of O_2 followed by 5 L of CO at 90 K and flashed to 273 K to desorb CO_2. The intensity of the XPS peak located at 289 eV, assigned to carbonate, clearly decreases when Au coverage is increased. The absence of the peak at 289 eV for the Au/Ni(111) prepared with the highest Au coverage furthermore demonstrates that it is possible to completely block the carbonate formation if the Au coverage is above 0.5 ML. At this high Au coverage we only observe one peak at 286.1 eV assigned to CO chemisorbed in on-top Ni-sites. The intensity of this peak is identical before (not shown) and after a flash to 273 K, and from this we conclude that the 0.5 ML Au/Ni(111) surface alloy is inactive for low-temperature CO oxidation.

The observed CO_2 TPD spectrum taken on the Au/Ni(111) surface alloy with 43% Au looks similar to the one observed previously by Lahr and Ceyer,[4] who suggested the existence of a unique molecular O_2 adsorption state stabilized by the presence of Au atoms on the Ni(111) surface. Exothermic dissociation of this molecular oxygen upon heating was proposed to lead to CO_2 formation *via* a "hot" atom mechanism on Au/Ni(111) surfaces. Our TPD measurements suggest that the low-temperature adsorption of O_2 on Ni(111) and Au/Ni(111) surfaces and the reactivity of these surfaces toward CO are qualitatively similar, indicating that the role of Au is perturbative in nature. The similarity of O_2 adsorption on these two surfaces is corroborated by our XPS data in which the O 1s regions of the oxygen saturated Ni(111) surface and Au/Ni(111) surface alloy appear to be very similar. The difference between our results demonstrating low-temperature CO oxidation catalyzed by NiO_x and the low-temperature CO oxidation observed by Lahr and Ceyer[4] caused by the stabilization of molecular oxygen on Au atoms within the Au−Ni alloy might be explained by the very different oxygen exposures employed in the experiments. Since Lahr and Ceyer only dosed approximately 3 L of O_2 at 77 K, it is unlikely that NiO_x formed under their experimental conditions (Sylvia Ceyer, personal communication), while our experiments clearly reveal that nickel oxide is formed after exposures of >100 L of oxygen onto the Ni(111) surface or the Au/Ni(111) surface alloy. Thus, in the Lahr and Ceyer studies the role of Au may be decisive and not perturbative as it is on NiO_x.

Mechanism for Low-Temperature CO Oxidation. To rationalize and gain further insights into the mechanism of the experimentally observed low-temperature CO oxidation on Ni(111), we used DFT calculations to study the CO oxidation on a series of model surfaces: (i) submonolayer and full-monolayer oxygen chemisorption structures on Ni(111) surfaces, (ii) Ni(111) surfaces with local O islands, and (iii) NiO(111) surfaces. These DFT calculations will be presented in more detail in a separate publication.

The DFT-calculated activation energy barriers for CO oxidation on $^1/_3$ ML and $^2/_3$ ML O-predosed Ni(111) surfaces are 0.83 and 0.79 eV, respectively. On a full-monolayer O-covered Ni(111) surface, and in the case that CO reacts off the preadsorbed O directly above an fcc site (Eley−Rideal mechanism), an activation energy barrier of *ca.* 1.2 eV was obtained. However, when the incoming CO(g) approaches the preadsorbed O atom (at an fcc site) from above a neighboring bridge site, the barrier was reduced to 0.5 eV. All of these barriers are too high to explain the observed CO oxidation at ~120 K. For a reaction to take place at a reasonable rate at this low temperature the barrier would have to be of the order ~0.2 eV or less.

Also, CO oxidation on a large Ni(111) surface with local O-islands is found to be energetically difficult. In particular, the activation energy barrier for CO oxidation on a (2 × 2) O-island formed on a Ni(111)-(6 × 6) surface unit cell is at least 1.0 eV. These results suggest that chemisorbed O on Ni(111) structures (submonolayer O preadsorbed Ni(111), O islands on Ni(111), or a full-monolayer O-covered Ni(111)) cannot be the active phase responsible for the low-temperature (~120 K) CO oxidation observed in our experiments.

As discussed in previous sections, local nickel-oxide islands are formed when a large amount of O_2 was dosed on Ni(111). The STM results image a great deal of structural disorder, and this fact, together with the mismatched lattice constants of Ni and NiO (which necessitate large unit cells in periodic calculations), makes an exact treatment of the experimentally observed system intractable for our DFT methods. As a suitable model system for the experimentally observed NiO islands we have used the NiO(111) surface of bulk NiO. The pristine NiO(111) surface is unstable due to its polar structure, and readily reconstructs into the O-terminated octopolar NiO(111) surface, and thus we have used this surface for our DFT calculations.

An advantageous feature of the octopolar NiO(111) surface reconstruction is that it exposes undercoordinated Ni sites. Such sites are likely to be present on a defective NiO surface, and we therefore tentatively suggest that they are also present in the structurally disordered NiO islands observed in the STM images. These defect sites may play a crucial role in the observed CO oxidation by providing adsorption sites for molecular oxygen. To explain the experimental observations, we have examined different configurations in which (1) molecular O_2 can be stabilized, and (2) pathways leading to CO_2 formation with small or vanishing barriers exist.

We find from extensive DFT calculations that on a clean O-terminated octopolar NiO(111) surface, CO prefers to bond to a Ni-atop site, with a modest binding energy of −0.46 eV. However, CO oxidation on the clean octopolar NiO(111) surface using a crystal apex O atom as a reactant is energetically very demanding. In contrast, when O_2 was preadsorbed on the NiO(111) surface at a sufficiently high coverage so that all surface Ni atoms are blocked by oxygen, our DFT calculations showed that the NiO apex O atom can spontaneously react with CO (see Figure 6). Yet, the CO_2 product from this reaction is only weakly bound on the O_2 preadsorbed defective NiO(111) (the defect is created after reacting off the apex O), and the energy needed for CO_2 desorption from the surface is 0.47 eV. We tentatively suggest that desorption of this surface bound CO_2 may occur at low temperature assisted by the energy release from chemisorption and/or dissociation of a nearby O_2 molecule. In particular, the DFT calculations show that the binding of O_2 to the vacancy created upon CO_2 desorption is exothermic by 0.94 eV. Following a healing of the O-apex vacancy by CO_2 desorption and O_2 adsorption, our DFT calculations show that the extra O atom atop of the apex-O is removed by spontaneous reaction with another CO molecule, and thus the DFT calculations appear to suggest a closed catalytic CO oxidation cycle. A detailed discussion of the DFT model and the DFT calculations will be presented in a separate publication.

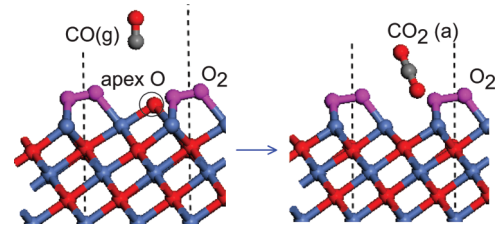

Figure 6. On the NiO(111) surface preadsorbed by O_2, the apex O atom of NiO(111) can spontaneously react with CO, forming CO_2, which is weakly bound on the surface. Blue, red, and gray spheres represent Ni, O, and C, respectively. The preadsorbed O_2 are highlighted by magenta spheres.

CONCLUSIONS

We have shown that a small amount of CO_2 is produced at ~100 K on both Ni(111) surfaces and Au/Ni(111) surface alloys in the presence of loosely bound oxygen. The STM and XPS results indicate that nickel oxide is formed on both the pure Ni(111) surface and Au/Ni(111) surface alloys at ~100 K. Our TPD measurements reveal increased low-temperature CO_2 formation upon addition of Au, and both TPD and XPS show that Au inhibits carbonate formation. DFT model calculations identify barrierless pathways to CO_2 formation on defective NiO_x surfaces upon saturation with O_2, and we suggest that nickel oxides play a central role in catalyzing CO oxidation at cryogenic temperatures.

EXPERIMENTAL AND THEORETICAL METHODS

The Ni(111) crystal was cleaned by multiple cycles of Ar-sputtering (2 keV) at room temperature and annealing to 800 or 1000 K until no contamination could be detected with the STM or XPS. STM measurements were carried out at temperatures between 100−350 K with the home-built Aarhus-STM[17] mounted in a UHV chamber with base pressure ~1×10^{-10} Torr. For the STM measurements the temperature was measured with a type-K thermocouple in mechanical contact with the crystal. Au was deposited onto Ni(111) at room temperature from a home-built thermal evaporator or a commercial E-beam evaporator. Subsequent annealing at 800 K for 10 min led to the formation of the Au/Ni(111) surface alloy where individual Au atoms are substituted into the Ni(111) surface layer. In the STM chamber the evaporators were calibrated from STM images of Au deposition at room temperature onto the Ni(111) surface, in which case Au grows pseudomorphic into large Au-islands.[18]

CO, O_2, and CO_2 gas exposures are given in langmuir (1.0×10^{-6} Torr · s), and they are based on the ion gauge reading with no correction for different sensitivity factors of the gases. In the STM chamber the Ni(111) crystal was oxidized by exposing the single crystal to O_2 at low temperatures (100 K) when the sample was located in the STM. When the sample is in the STM, the local pressure on the sample surface is lower than the measured pressure in the chamber, the reason being the cold Al block of the STM in which the scanner tube is mounted. When cooled to 100 K, the Al block acts as a small cryopump. In the TPD setup, the Ni(111) crystal was supported by W wires. These W wires were also used for resistively heating of the crystal. A thermocouple was spot-welded to the side of the crystal, and a feedback circuit was used to control the temperature of the crystal with high precision. The tungsten wire was in mechanical contact with a liquid nitrogen Dewar and temperatures below 100 K could be reached in the TPD setup. Au coverages in the TPD setup were measured indirectly by the CO-desorption experiments. CO molecules adsorbed at RT will only adsorb on the Ni(111) surface, and the integrated CO desorption signal is thus proportional to the area of Au-free Ni(111) surface. All TPD experiments were performed with a linear heating rate of 1 K/s. The TPD spectra were recorded directly after gas dosing, and the background signal was fitted with a polynomial and subtracted from each spectrum. Desorbed quantities were calculated by the integration of the TPD spectra using the known saturation coverage of CO at RT (0.5 ML)[19] and gas sensitivity factors for the mass spectrometer.

The XPS measurements were performed at MAX-Lab, beamline I311, which is described in detail elsewhere.[20] The XPS spectra, which were collected in normal emission with photon energies of 380 eV for C 1s and 625 eV for O 1s levels, are normalized directly to the beam current in the storage ring or to the spec-

trum background, and the binding energies are calibrated to the Fermi edge. Asymmetric Voigt peaks are used for the curve fitting, and CO and oxygen coverages are determined by integration. In the XPS chamber the Au doser was calibrated by measuring the Au 4f peak after deposition of Au on a Ru(0001) crystal.[21]

Periodic DFT calculations were performed with the Vienna *ab-initio* simulation package (VASP) code,[22] using ultrasoft pseudopotentials or projected augmented wave (PAW) potentials.[23,24] The exchange-correlation functional was described by the generalized gradient approximation,[25] and an energy cutoff of 400 eV was used. The Ni(111) surface was modeled by a four-layer slab with a $(\sqrt{3} \times \sqrt{3})$R30° surface unit cell. The NiO(111) surface was modeled by a slab with six NiO double-layers with the p(2 × 2) O-terminated octopolar reconstruction ($^3/_4$ ML O missing in the top layer and $^1/_4$ ML Ni missing in the second layer).[26,27] For modeling reactivity on NiO(111), the DFT+*U* method[28] with the parameters of $U = 6.3$ eV and $J = 1$ eV[29] for Ni 3d orbitals was used. The two bottom-most Ni layers for Ni(111) or NiO double-layers for NiO(111) were kept fixed during calculations; the remaining layers of the slab, including the absorbate, were allowed to relax. More details on these calculations can be found in a forthcoming publication.

Acknowledgment. The authors thank the Danish Research Agency, the Danish Strategic Research Council, the Danish Council for Independent Research, the Carlsberg Foundation, the Villum Kahn Rasmussen Foundation, and the European Research Council for financial support. Work at the University of Wisconsin-Madison was supported by DOE-BES, Division of Chemical Sciences. CPU time was utilized at facilities located at NERSC, ORNL, PNNL, and ANL, all supported by the US-DOE. Sylvia Ceyer is gratefully acknowledged for sharing with us additional information and for enlightening discussions on her HREELS measurements on the Au/Ni(111) surface alloy.

REFERENCES AND NOTES

1. Besenbacher, F.; Chorkendorff, I.; Clausen, B. S.; Hammer, B.; Molenbroek, A. M.; Norskov, J. K.; Stensgaard, I. Design of a Surface Alloy Catalyst for Steam Reforming. *Science* **1998**, *279*, 1913–1915.
2. Nielsen, L. P.; Besenbacher, F.; Stensgaard, I.; Laegsgaard, E.; Engdahl, C.; Stoltze, P.; Jacobsen, K. W.; Norskov, J. K. Initial Growth of Au on Ni(110)—Surface Alloying of Immiscible Metals. *Phys. Rev. Lett.* **1993**, *71*, 754–757.
3. Holmblad, P. M.; Larsen, J. H.; Chorkendorff, I. Modification of Ni(111) Reactivity Toward CH_4, CO, and D_2 by Two-Dimensional Alloying. *J. Chem. Phys.* **1996**, *104*, 7289–7295.
4. Lahr, D. L.; Ceyer, S. T. Catalyzed CO Oxidation at 70 K on an Extended Au/Ni Surface Alloy. *J. Am. Chem. Soc.* **2006**, *128*, 1800–1801.
5. Tyuliev, G. T.; Kostov, K. L. XPS/HREELS Study of NiO Films Grown on Ni(111). *Phys. Rev. B* **1999**, *60*, 2900–2907.
6. Kitakatsu, N.; Maurice, V.; Hinnen, C.; Marcus, P. Surface Hydroxylation and Local Structure of NiO Thin Films Formed on Ni(111). *Surf. Sci.* **1998**, *407*, 36–58.
7. Kim, C. M.; Jeong, H. S.; Kim, E. H. NEXAFS and XPS Characterization of Molecular Oxygen Adsorbed on Ni(100) at 80 K. *Surf. Sci.* **2000**, *459*, L457–L461.
8. Schulze, M.; Reissner, R.; Bolwin, K.; Kuch, W. Interaction of Water with Clean and Oxygen Precovered Nickel Surfaces. *Fresenius' J. Anal. Chem.* **1995**, *353*, 661–665.
9. Held, G.; Schuler, J.; Sklarek, V.; Steinruck, H. P. Determination of Adsorption Sites of Pure and Coadsorbed CO on Ni(111) by High Resolution X-ray Photoelectron Spectroscopy. *Surf. Sci.* **1998**, *398*, 154–171.
10. Cappus, D.; Xu, C.; Ehrlich, D.; Dillmann, B.; Ventrice, C. A.; Alshamery, K.; Kuhlenbeck, H.; Freund, H. J. Hydroxyl-Groups on Oxide Surfaces—NiO(100), NiO(111) and Cr_2O_3(111). *Chem. Phys.* **1993**, *177*, 533–546.
11. Badyal, J. P. S.; Zhang, X. K.; Lambert, R. M. A Model Oxide Catalyst System for the Activation of Methane−Lithium-Doped NiO on Ni(111). *Surf. Sci.* **1990**, *225*, L15–L19.
12. Chiarello, G.; Cupolillo, A.; Giallombardo, C.; Agostino, R. G.; Formoso, V.; Pacile, D.; Papagno, L.; Colavita, E. Co-adsorption of Oxygen and Carbon Monoxide on Ni(111). *Surf. Sci.* **2003**, *536*, 33–44.
13. Behm, R. J.; Brundle, C. R. On the Formation and Bonding of a Surface Carbonate on Ni(100). *Surf. Sci.* **1991**, *255*, 327–343.
14. Li, W.; Stirniman, M. J.; Sibener, S. J. Electron-Stimulated Oxidation of Ni(111) at Low Temperature. *Surf. Sci.* **1995**, *329*, L593–L598.
15. Gordon, D. E. A.; Lambert, R. M. CO_2 Adsorption on Oxygen-Modified Ni(111). *Surf. Sci.* **1993**, *287*, 114–118.
16. Guo, X. C.; Yoshinobu, J.; Yates, J. T. Photon-Induced Desorption of CO Chemisorbed on the Oxidized Ni(111) Surface. *J. Chem. Phys.* **1990**, *92*, 4320–4326.
17. Laegsgaard, E.; Besenbacher, F.; Mortensen, K.; Stensgaard, I. A Fully Automated, Thimble-Size Scanning Tunnelling Microscope. *J. Microsc.* **1988**, *152*, 663–669.
18. Jacobsen, J.; Nielsen, L. P.; Besenbacher, F.; Stensgaard, I.; Laegsgaard, E.; Rasmussen, T.; Jacobsen, K. W.; Norskov, J. K. Atomic-Scale Determination of Misfit Dislocation Loops at Metal−Metal Interfaces. *Phys. Rev. Lett.* **1995**, *75*, 489–492.
19. Netzer, F. P.; Madey, T. E. The Structure of CO on Ni(111). *J. Chem. Phys.* **1982**, *76*, 710–715.
20. Nyholm, R.; Andersen, J. N.; Johansson, U.; Jensen, B. N.; Lindau, I. Beamline I311 at MAX-LAB: A VUV/soft X-ray Undulator Beamline for High Resolution Electron Spectroscopy. *Nucl. Instrum. Methods Phys. Res.* **2001**, *467*, 520–524.
21. Potschke, G.; Schroder, J.; Gunther, C.; Hwang, R. Q.; Behm, R. J. A STM Investigation of the Nucleation and Growth of Thin Cu and Au Films on Ru(0001). *Surf. Sci.* **1991**, *251*, 592–596.
22. Kresse, G.; Furthmuller, J. Efficient Iterative Schemes for *ab Initio* Total-Energy Calculations Using a Plane-Wave Basis Set. *Phys. Rev. B* **1996**, *54*, 11169–11186.
23. Blochl, P. E. Projector Augmented-Wave Method. *Phys. Rev. B* **1994**, *50*, 17953–17979.
24. Kresse, G.; Joubert, D. From Ultrasoft Pseudopotentials to the Projector Augmented-Wave Method. *Phys. Rev. B* **1999**, *59*, 1758–1775.
25. Perdew, J. P.; Wang, Y. Accurate and Simple Analytic Representation of the Electron-Gas Correlation Energy. *Phys. Rev. B* **1992**, *45*, 13244–13249.
26. Wolf, D. Reconstruction of NaCl Surfaces from a Dipolar Solution to the Madelung Problem. *Phys. Rev. Lett.* **1992**, *68*, 3315–3318.
27. Barbier, A.; Mocuta, C.; Kuhlenbeck, H.; Peters, K. F.; Richter, B.; Renaud, G. Atomic Structure of the Polar NiO(111)-p(2 × 2) Surface. *Phys. Rev. Lett.* **2000**, *84*, 2897–2900.
28. Dudarev, S. L.; Botton, G. A.; Savrasov, S. Y.; Humphreys, C. J.; Sutton, A. P. Electron-Energy-Loss Spectra and the Structural Stability of Nickel Oxide: An LSDA+*U* Study. *Phys. Rev. B* **1998**, *57*, 1505–1509.
29. Rohrbach, A.; Hafner, J.; Kresse, G. Molecular Adsorption on the Surface of Strongly Correlated Transition-Metal Oxides: A Case Study for CO/NiO(100). *Phys. Rev. B* **2004**, *69*, 075413.